L-asparaginase encapsulation into asymmetric permeable polymersomes

Cecilia Z. Bueno, †, ‡ Alexsandra C. Apolinário †, ‖, ‡, Aroa Duro-Castano ‡, Alessandro Poma ‡, ⊣, Adalberto Pessoa-Jr, † Carlota O. Rangel-Yagui, *, † Giuseppe Battaglia *, ‡, §, ⊥

† Department of Biochemical and Pharmaceutical Technology, University of São Paulo, 05508-000, São Paulo, Brazil

‖ Department of Pharmacology, University of São Paulo, 05508-000, São Paulo, Brazil

‡ Department of Chemistry, University College London, WC1H 0AJ, London, United Kingdom

⊣ Eastman Dental Institute, University College London, WC1X 8LD, London, United Kingdom

§ Institute for Bioengineering of Catalonia (IBEC), 08028, Barcelona Institute for Science and Technology (BIST), 08036, Barcelona, Spain

⊥ Catalan Institution for Research and Advanced Studies, (ICREA), 08010, Barcelona, Spain

ABSTRACT: This work reports for the encapsulation of L-asparaginase, an anticancer enzyme into hybrid $PMPC_{25}$-$PDPA_{70}$/ PEO_{16}-PBO_{22} asymmetric polymersomes previously developed by our group, with loading capacities with over than 800 molecules per vesicle. Enzyme-loaded polymersomes show permeability and capacity to hydrolyze L-asparagine, which is essential to cancer cells. The nanoreactors proposed in this work can potentially be used in further studies to develop novel therapeutic alternatives based on L-asparaginase.

L-asparaginase, also called L-asparagine amidohydrolase (ASNase), is an important enzyme used to treat leukaemias and lymphomas due to its catalytic activity in the hydrolysis of L-asparagine to L-aspartate and ammonia. L-asparagine (Asn) depletion by ASNase results in starvation and death of cancer cells, which are dependent on the exogenous supply of this amino acid. Normal cells, on the other hand, are not affected because of their ability to synthesize Asn [1–6]. L-asparaginase has also been studied for the treatment of other malignancies and proved to reduce metastasis in a model of breast cancer [7] and to suppress melanoma and pancreatic cancer growth when in combination with MEK inhibitor [8]. Currently, four ASNase formulations are commercialized, three from *Escherichia coli* (native, recombinant and PEGylated) and one from *Dickeya chrysanthemi*. The *E.coli* non-PEGylated enzyme is the most used in chemotherapy [9].

Unfortunately, ASNase-based therapy has some limitations due to the production of ASNase antibodies and the presence of proteases which shortens its *in vivo* half-life, leading to repeated administrations and to allergic reactions [6]. Also, ASNase secondary L-glutaminase activity leads to adverse symptoms. Some possible reactions include skin rashes, oedema, bronchospasm, hepatotoxicity, neurotoxicity, coagulation and respiratory disorders, pancreatitis, hyperglycaemia, low blood pressure as well as anaphylactic shock [1,3,4].

In this context, ASNase nanoencapsulation as long as its enzymatic activity is preserved appears as an alternative to protect the enzyme against proteases and antibodies, providing sustained active concentration and improving stability, bioavailability and biocompatibility [9]. The literature already reports studies of ASNase nanoencapsulation, such as in polymeric nanoparticles,[10–19] in liposomes [20–23]. However, there are no formulations currently in use in the clinical practice [5]. Nanoencapsulation of ASNase into polymersomes (polymeric nanovesicles) holds great promise and appears as a good alternative. Only very few studies have reported this approach and for all the systems proposed the enzyme would have to be released for its action [9,24,25].

The polymersomes studied in this work are composed of a mixture of the copolymers poly[(2-methacryloyl) ethylphosphorylcholine]-poly[2-(diisopropylamino)ethyl methacrylate] (PMPC-PDPA) and poly(ethylene glycol) poly(butylene oxide) (PEO-PBO). PMPC-PDPA is a biocompatible and pH-sensitive copolymer [26]. The PDPA block becomes protonated under mildly acidic conditions (pKa = 6.5), which results in fast polymersomes disassembly [27]. PDPA-based polymersomes have been studied for the encapsulation and delivery of DNA, antibodies and anticancer drugs [27]. PEO-PBO is also biocompatible and forms very thin membranes which are permeable to small polar molecules [26]. The stealth property of the PEO chain reduces cellular uptake and increases circulation time in the blood stream [28]. At an optimal molar ratio of 90% PMPC-PDPA to 10% PEO-PBO, asymmetric nanovesicles with separated membrane domains are obtained, containing a small permeable bud formed by the minor PEO-PBO constituent [26,29].

The asymmetric permeability of 90% PMPC-PDPA and 10% PEO-PBO polymersomes to small polar molecules, such as Asn, is explored for ASNase encapsulation. Therefore, this novel system could potentially be employed to the depletion of the circulating amino acid Asn from the blood stream while maintaining the enzyme encapsulated for a prolonged time. A schematic representation of the system is shown in Figure 1.

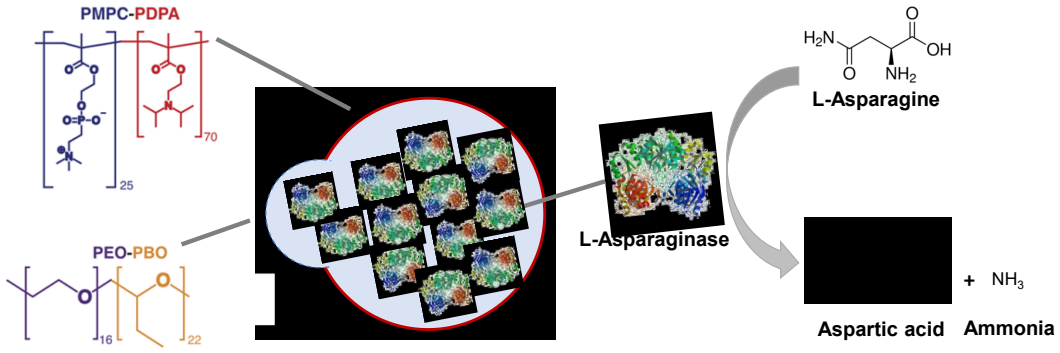

Figure 1. Schematic representation of an asymmetric polymersome formed by a combination of 9:1 PMPC-PDPA/PEO-PBO encapsulating L-asparaginase. The hydrolisis of L-asparagine into aspartate and ammonia is shown on the right.

In this study three different polymersome formulations are prepared: 90% PMPC-PDPA/10% PEO-PBO (90:10) and the controls consisting of 100% PMPC-PDPA (100:0) and 100% PEO-PBO (0:100). All polymersome formulations are prepared by the film hydration method [26].

The enzyme ASNase is encapsulated through electroporation with an initial voltage of 2500 V and resulting voltage of around 700 V, employing 10 or 20 pulses with an interval of 60 s between each pulse. The systems are purified by size-exclusion chromatography (SEC) [30] to remove non-encapsulated enzyme (Supplementary Info. S1).

Asymmetric polymersomes of PMPC-PDPA and PEO-PBO and symmetric polymersomes formed only by PMPC-PDPA present similar size distributions by number, with mean diameters around 104 nm to 120 nm, as shown in Figure 2. The observed diameters can be considered adequate to achieve long-circulation times in the bloodstream, according to studies performed with polybutadiene-poly(ethylene glycol) polymersomes [31,32]. Polydispersity index (PdI), which is a dimensionless parameter between 0 and 1 used to describe the degree of heterogeneity of a size distribution of particles [33], are below 0.3 for all samples, being lower for asymmetric vesicles, which indicates homogeneous populations.

ASNase loaded samples do not differ significantly in size compared to the control (empty) vesicles, indicating preservation of the polymersome structure after electroporation. Moreover, empty and loaded vesicles present good stability after two months (Supplementary Info. S3). Pure PEO-PBO polymersomes are also analysed by dynamic light scattering (DLS) and presented good stability (Supplementary Info. S4).

Transmission electron microscopy (TEM) of single vesicles and of the vesicle populations are shown in Figure 2 (A3, A4, B3, B4). Symmetric polymersomes present spherical morphology, whereas asymmetric polymersomes present a small bud of PEO-PBO, as previously demonstrated by our group [26,29]. Asymmetric vesicles are a stable single compartment, with different copolymer domains at the surface [29].

Enzyme loading by electroporation does not change the morphology, consistent with another study with PMPC-PDPA polymersomes [34], indicating that the vesicles self-heal after the application of high voltages. The morphology of pure PEO-PBO vesicles analysed by TEM are shown in the Supplementary Information S4.

Lower magnification TEM images (Figure 2: A5, B5) show that all nanoparticle populations present mixed morphologies, including spherical and tubular vesicles. The latter ones are transitional structures that eventually "pearl" into smaller tubes and spherical polymersomes [30]. The same results were observed by our group in the production of PMPC-PDPA polymersomes by film hydration [30,35].

It is important to note that the heterogeneity of the polymersome populations is maintained even after SEC purification since this technique is employed only to remove non-encapsulated ASNase, and the purified polymersome fractions are collected into a single vial. The effectiveness of SEC purification in separating non-encapsulated enzyme is confirmed by Micro-BCA protein concentration assay, as shown in Supplementary Information S4.

TEM images of single asymmetric vesicles stained with PTA are analysed using ImageJ Software, as shown in Figure 3. Magnification of the micrograph facilitates distinguishing between the darker PMPC-PDPA domains and the lighter PEO-PBO domains [29] (Figure 3A). The hydrophobic thickness of both copolymers is measured by plotting the intensity profile vs distance and observing the intensity drop corresponding to the darkest regions [26]. Intensity plots indicate an average membrane thickness of 6.8 nm for PMPC-PDPA domain (Figure 3B) and 2 nm for PEO-PBO domain (Figure 3C). Similar values (6.4 nm for PMPC-PDPA and 2.4 nm for PEO-PBO) were found by Joseph et al. (2017) [26]. The micrographs are also filtered using the LUT (Lookup Tables) tool of ImageJ Software, which enables better highlighting of the polymeric membrane and background removal (Figure 3D).

ASNase encapsulation into symmetric and asymmetric polymersomes is performed through electroporation. The method is verified with the pure enzyme, which is electroporated in the presence of PBS (pH 7.4) and analysed by the enzymatic Nessler assay. Activity losses of 11.5% and 19.4% are observed after electroporation with 10 and 20 pulses, respectively. Therefore, the enzyme retains most of its activity even after exposition to a high 2500 V initial voltage.

It is important to add that ASNAse encapsulation depends mostly on the polymersomes membrane composition and thickness, since the applied electric pulses must be able to disturb the structure creating temporary pores that allow enzyme entrapment [34]. Therefore, the vesicles size and shape are not expected to significantly affect the enzyme loading.

Table 1 shows the results of ASNase encapsulation into symmetric and asymmetric polymersomes. All parameters are calculated following Wang et al. (2012) [34] (Supplementary Info. S6).

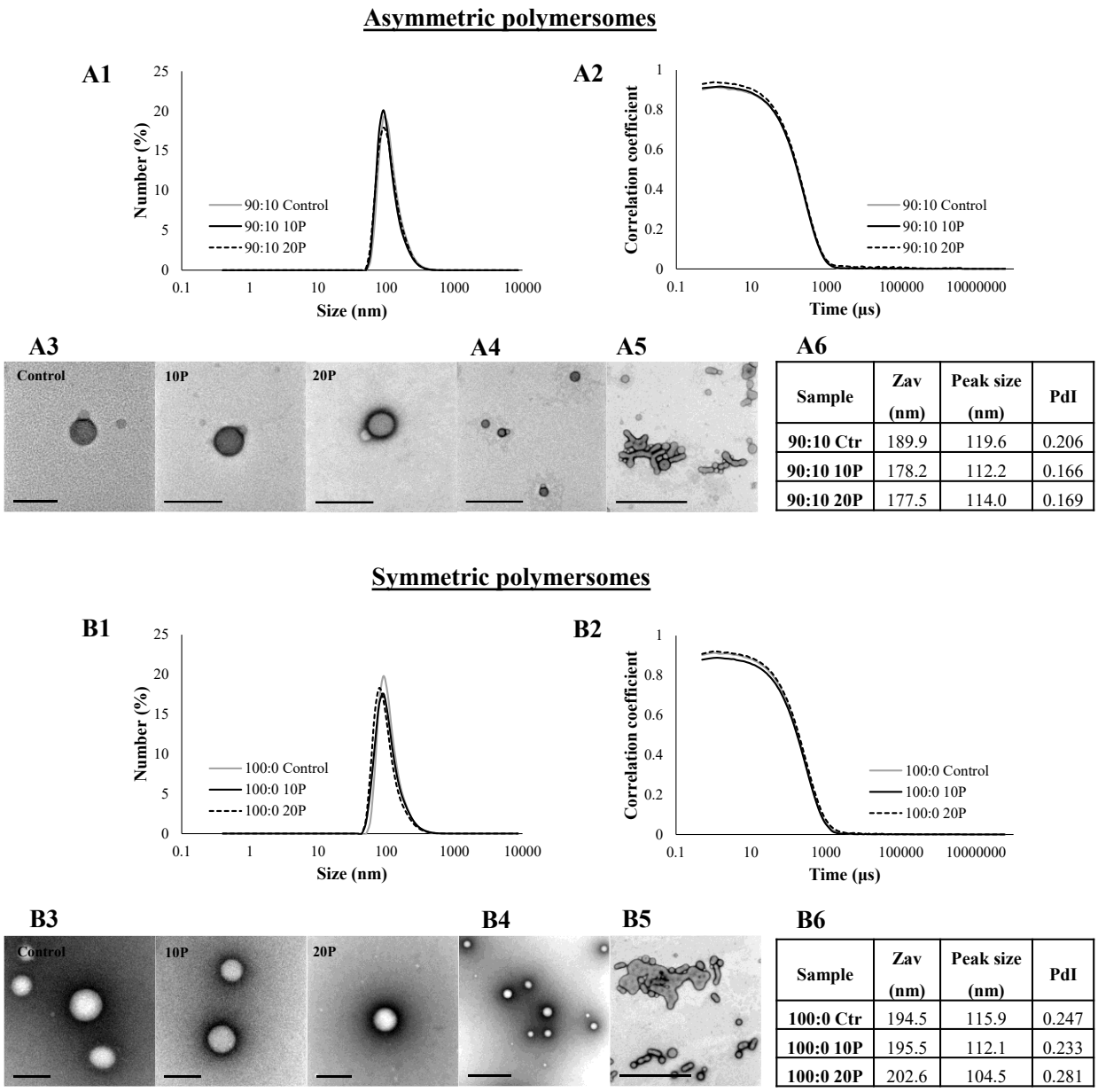

Figure 2. Size distribution and morphology of symmetric (100:0) and asymmetric (90:10) polymersomes encapsulating ASNase by electroporation using 10 pulses (10P) or 20 pulses (20P). (**A1, B1**) Number distribution measured by dynamic light scattering (DLS). (**A2, B2**) DLS correlation function. (**A3, B3**) Transmission electron microscopy (TEM) images of single vesicles (25000 X). (**A4, B4**) Transmission electron microscopy (TEM) images at lower magnification (7000 X). (**A5, B5**) TEM images of the mixed morphology vesicles populations (5000 X). (**A6, B6**) Z-average particle size, peak size of number distribution and polydispersity index (PdI) obtained by DLS.

To verify if the measured ASNase was indeed encapsulated, another experiment is performed mixing an electroporated enzyme solution with a non-electroporated symmetric polymersome system. After purifying by SEC and breaking the vesicles in acidic pH, the system is analysed in HPLC. The results indicate encapsulation efficiencies of 0.7-1.0% and loading capacities of 37-54 molecules/polymersome (Supplementary Info. S7), which represents about 10-21% of the calculated loading capacities of Table 1. The amounts of ASNase detected in this experiment can be attributed to large aggregates that elute together with the polymersomes in the SEC column and should be accounted for as an experimental error.

The actual loading/theoretical loading values are considerably higher than unit, suggesting a positive interaction between ASNase and polymersomes [34]. On the other hand, the polymersome production efficiencies indicate significant loss of polymer during preparation, in accordance with the visible polymeric bulk formed during the first centrifugation step of the film hydration method (Supplementary Info. S1).

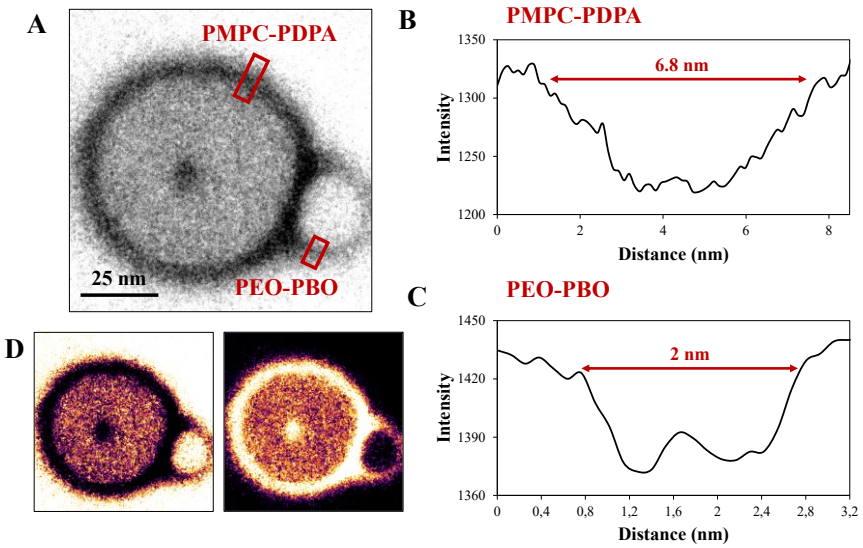

Figure 3. Thickness analysis. (**A**) TEM of an asymmetric polymersome indicating the sites chosen for thickness measurement. (**B**) Intensity profile of PMPC-PDPA and corresponding thickness value. (**C**) Intensity profile of PEO-PBO and corresponding thickness value. (**D**) Lookup Tables (LUT) filtered and inverse LUT filtered micrographs obtained with ImageJ software.

Table 1. ASNase encapsulation results for symmetric and asymmetric polymersomes.

Sample	Actual loading/theoretical loading (mg/mg)[a]	Polymersome production efficiency (%)[b]	Encapsulation efficiency (%)[c]	Loading capacity[d]
90:10 10P	33.3	63.3	8.8	741
90:10 20P	55.3	43.4	10.0	845
100:0 10P	36.5	55.2	6.6	252
100:0 20P	36.7	49.8	7.8	364

a) ratio between the actual mass of loaded enzyme and the theoretical loading [34]; b) percentage of polymer that formed polymersomes; c) percentage of the initial amount of enzyme that is encapsulated; d) average number of ASNase molecules per vesicle.

90:10 – asymmetric polymersomes; 100:0 – symmetric polymersomes; 10P, 20P – number of electroporation pulses

Asymmetric (90:10) polymersomes have higher encapsulation efficiencies and loading capacities than symmetric (100:0) polymersomes. This is attributed to differences in the voltage required for effective electroporation between the formulations. Aranda-Espinoza et al. (2001) [36] defined that the required voltage or, in other words, the membrane breakdown potential, is directly proportional to the membrane thickness. Therefore, the presence of a thinner and more permeable PEO-PBO membrane region decreases the total breakdown potential and increases electroporation efficiency.

The increase in the number of pulses results in increased encapsulation efficiency and loading capacity. Also, Wang et al. (2012) [34] observed that increasing the number of pulses considerably increased BSA and IgG loading into PMPC-PDPA polymersomes. The authors also observed that the applied voltage had almost no effect on the encapsulation efficiency.

The calculated ASNase encapsulation efficiency values ranged from 6.6 to 10%. Similar values are found in the literature for ASNase encapsulated into poly(2-hydroxypropyl methacrylate) (PHPMA) polymersomes comprised of a PEG shell. In this work, vesicle production and ASNase encapsulation were performed simultaneously through aqueous photo-polymerization-induced self-assembly (PISA), resulting in an encapsulation efficiency of 9% [25]. In another work, ASNase was encapsulated into Pluronic® L-121 polymersomes produced by temperature switch with an efficiency of 5% [9]. ASNase was also encapsulated into PEG-PLA polymersomes with efficiencies in the range 7.5 to 25%, however, as observed by the authors, these values might be overestimated because the protein was quantified in the supernatant after centrifugation of the system [9,24]. The relatively low encapsulation efficiency values for ASNase in polymersomes result from the fact that the protein is passively incorporated inside the vesicles with no specific interactions. In other words, the encapsulation efficiency depends on the initial enzyme concentration and the total internal volume of the vesicles.

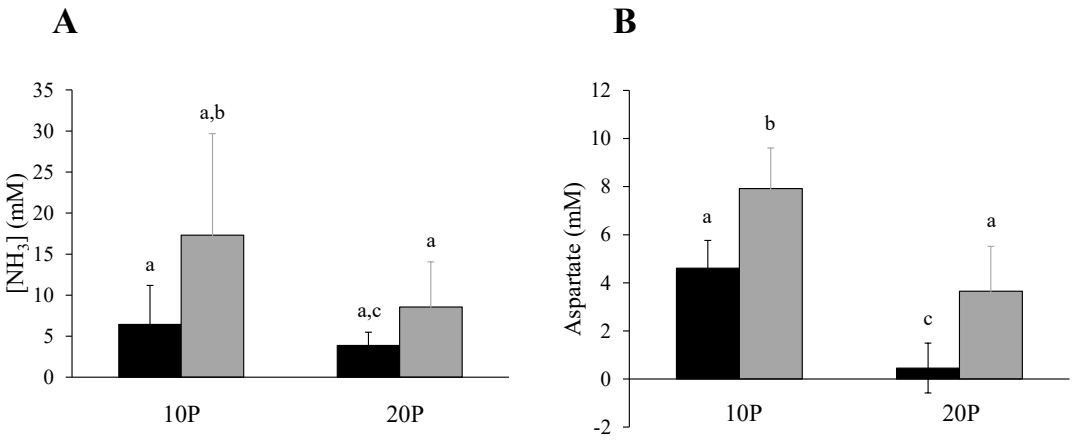

Figure 4. Enzymatic activity of ASNase loaded polymersomes based on ammonia and aspartate production. (**A**) Nessler Assay. (**B**) Aspartate Assay. (■) Symmetric polymersomes. (■) Asymmetric polymersomes. Different letters indicate significant difference (Tukey test, $p<0.05$).

Despite the relatively low encapsulation efficiency values, the calculated loading capacities are high (252 to 364 for symmetric and 741 to 845 for asymmetric vesicles). This result is probably due to the use of an excess of ASNase. Other authors report lower ASNase loading capacities, for example, the enzyme encapsulation by vortex and mixing in PICsomes (polyion complex vesicles) of PEG-poly(α,β-aspartic acid) (PEG-b-P(Asp) and poly([5-aminopentyl]-α,β-asoartamide) (P(Asp-AP) resulted in approximately two ASNase molecules per vesicle [37].

The activity of encapsulated ASNase is measured regarding ammonia and aspartate production after incubating the systems with Asn and quantifying protein by micro-BCA [38] and activity by Nessler assay [39].

The results shown in Figure 4 reveal that both ammonia and aspartate concentrations tend to be higher for asymmetric polymersomes, which is attributed to their higher permeability due to the PEO-PBO bud and to their higher loading capacities. Statistically significant differences were observed more often in the aspartate assay, according to the Tukey test. Additionally, both symmetric and asymmetric samples loaded with 10 pulses present higher activity. This result is probably due to the decrease of the enzymatic activity with the increase in the number of pulses applied, as discussed previously.

In conclusion, ASNase was successfully encapsulated into asymmetrically permeable polymersomes with high loading capacities and the resulting system was proved to deplete Asn from the external medium while keeping the enzyme inside the vesicles. The concept proposed in this work could be employed in futher studies to develop novel ASNase platforms as nanoreactors for the treatment of blood malignancies originated in the bone marrow. Future work is still needed to achieve a biodegradable, highly biocompatible formulation, which needs to be thoroughly characterized regarding its *in vitro/in vivo* therapeutic efficiency and behaviour in the presence of proteases.

ASSOCIATED CONTENT

Supporting Information. S1: Materials and Methods; S2: NMR spectrum of PMPC-PDPA; S3: Polymersomes stability after 2 months; S4: PEO-PBO polymersomes characterization; S5: L-asparaginase purification by size exclusion chromatography; S6: Encapsulation results calculations; S7: Verification of ASNase encapsulation. This material is available free of charge via the Internet at http://pubs.acs.org.

AUTHOR INFORMATION

Corresponding Authors

* Carlota O. Rangel-Yagui. E-mail: corangel@usp.br
* Giuseppe Battaglia. E-mail: g.battaglia@ucl.ac.uk

Author Contributions

The manuscript was written through contributions of all authors. All authors have given approval to the final version of the manuscript.

Funding Sources

The authors received financial support by the São Paulo Research Foundation (FAPESP/Brazil) (grant numbers 2017/05272-0, 2016/16221-4 and 2013/08617-7) and the National Council for Scientific and Technological Development (CNPq/Brazil, Fellowship # 301832/2017-0).

Notes

The authors declare no competing financial interest.

ACKNOWLEDGMENT

The authors thank the Brazilian Nanotechnology National Laboratory (LNNano) for PEO-PBO polymersomes TEM images.

REFERENCES

(1) Lopes, A. M.; Oliveira-Nascimento, L. de; Ribeiro, A.; Tairum, C. A.; Breyer, C. A.; Oliveira, M. A. de; Monteiro, G.; Souza-Motta, C. M. de; Magalhães, P. de O.; Avendaño, J. G. F.; Cavaco-Paulo, A. M.; Mazzola, P. G.; Rangel-Yagui, C. de O.; Sette, L. D.; Converti, A.; Pessoa, A. Therapeutic L-Asparaginase: Upstream, Downstream and Beyond. *Crit. Rev. Biotechnol.* **2017**, *37 (1)*, 82–99.

(2) Tundisi, L. L.; Coêlho, D. F.; Zanchetta, B.; Moriel, P.; Pessoa, A.; Tambourgi, E. B.; Silveira, E.; Mazzola, P. G. L-Asparaginase Purification. *Sep. Purif. Rev.* **2017**, *46 (1)*, 35–43.

(3) Costa, I. M.; Schultz, L.; de Araujo Bianchi Pedra, B.; Leite, M. S. M.; Farsky, S. H. P.; de Oliveira, M. A.; Pessoa, A.; Monteiro, G. Recombinant L-Asparaginase 1 from Saccharomyces Cerevisiae:

An Allosteric Enzyme with Antineoplastic Activity. *Sci. Rep.* **2016**, *6 (1)*, 36239.

(4) Batool, T.; Makky, E. A.; Jalal, M.; Yusoff, M. M. A Comprehensive Review on L-Asparaginase and Its Applications. *Appl. Biochem. Biotechnol.* **2016**, *178 (5)*, 900–923.

(5) Brumano, L. P.; da Silva, F. V. S.; Costa-Silva, T. A.; Apolinário, A. C.; Santos, J. H. P. M.; Kleingesinds, E. K.; Monteiro, G.; Rangel-Yagui, C. de O.; Benyahia, B.; Junior, A. P. Development of L-Asparaginase Biobetters: Current Research Status and Review of the Desirable Quality Profiles. *Front. Bioeng. Biotechnol.* **2019**, *6 (JAN)*, 1–22.

(6) Maggi, M.; Mittelman, S. D.; Parmentier, J. H.; Colombo, G.; Meli, M.; Whitmire, J. M.; Merrell, D. S.; Whitelegge, J.; Scotti, C. A Protease-Resistant Escherichia Coli Asparaginase with Outstanding Stability and Enhanced Anti-Leukaemic Activity in Vitro. *Sci. Rep.* **2017**, *7 (1)*, 14479.

(7) Knott, S. R. V.; Wagenblast, E.; Khan, S.; Kim, S. Y.; Soto, M.; Wagner, M.; Turgeon, M.; Fish, L.; Erard, N.; Gable, A. L.; Maceli, A. R.; Dickopf, S.; Papachristou, E. K.; D'Santos, C. S.; Carey, L. A.; Wilkinson, J. E.; Harrell, J. C.; Perou, C. M.; Goodarzi, H.; Poulogiannis, G.; Hannon, G. J. Asparagine Bioavailability Governs Metastasis in a Model of Breast Cancer. *Nature* **2018**, *554 (7692)*, 378–381.

(8) Pathria, G.; Lee, J. S.; Hasnis, E.; Tandoc, K.; Scott, D. A.; Verma, S.; Feng, Y.; Larue, L.; Sahu, A. D.; Topisirovic, I.; Ruppin, E.; Ronai, Z. A. Translational Reprogramming Marks Adaptation to Asparagine Restriction in Cancer. *Nat. Cell Biol.* **2019**.

(9) Apolinário, A. C.; Ferraro, R. B.; de Oliveira, C. A.; Pessoa Jr, A.; de Oliveira Rangel-Yagui, C. Quality-by-Design Approach for Biological API Encapsulation into Polymersomes Using "Off-the-Shelf" Materials: A Study on L-Asparaginase. *AAPS PharmSciTech* **2019**, *20 (6)*, 251.

(10) Gaspar, M. M.; Blanco, D.; Cruz, M. E. M.; Alonso, M. J. Formulation of L-Asparaginase-Loaded Poly(Lactide-Co-Glycolide) Nanoparticles: Influence of Polymer Properties on Enzyme Loading, Activity and in Vitro Release. *J. Control. Release* **1998**, *52 (1–2)*, 53–62.

(11) Brito, A. E. M. de; Pessoa Jr, A.; Converti, A.; Rangel-Yagui, C. de O.; Silva, J. A. da; Apolinário, A. C. Poly (Lactic-Co-Glycolic Acid) Nanospheres Allow for High l-Asparaginase Encapsulation Yield and Activity. *Mater. Sci. Eng. C* **2019**, *98 (January)*, 524–534.

(12) Tinoco, A.; Ribeiro, A.; Oliveira, C.; Parpot, P.; Gomes, A.; Cavaco-Paulo, A. Albumin/Asparaginase Capsules Prepared by Ultrasound to Retain Ammonia. *Appl. Microbiol. Biotechnol.* **2016**, *100 (22)*, 9499–9508.

(13) Bahreini, E.; Aghaiypour, K.; Abbasalipourkabir, R.; Mokarram, A.; Goodarzi, M.; Saidijam, M. Preparation and Nanoencapsulation of L-Asparaginase II in Chitosan-Tripolyphosphate Nanoparticles and in Vitro Release Study. *Nanoscale Res. Lett.* **2014**, *9 (1)*, 340.

(14) Zhang, Y.-Q.; Wang, Y.-J.; Wang, H.-Y.; Zhu, L.; Zhou, Z.-Z. Highly Efficient Processing of Silk Fibroin Nanoparticle-l-Asparaginase Bioconjugates and Their Characterization as a Drug Delivery System. *Soft Matter* **2011**, *7 (20)*, 9728.

(15) Shakambari, G.; Sameer Kumar, R.; Ashokkumar, B.; Ganesh, V.; Vasantha, V. S.; Varalakshmi, P. Cloning and Expression of L-Asparaginase from Bacillus Tequilensis PV9W and Therapeutic Efficacy of Solid Lipid Particle Formulations against Cancer. *Sci. Rep.* **2018**, *8 (1)*, 18013.

(16) Muthukumar, T.; Chamundeeswari, M.; Prabhavathi, S.; Gurunathan, B.; Chandhuru, J.; Sastry, T. P. Carbon Nanoparticle from a Natural Source Fabricated for Folate Receptor Targeting, Imaging and Drug Delivery Application in A549 Lung Cancer Cells. *Eur. J. Pharm. Biopharm.* **2014**, *88 (3)*, 730–736.

(17) Ortac, I.; Simberg, D.; Yeh, Y.; Yang, J.; Messmer, B.; Trogler, W. C.; Tsien, R. Y.; Esener, S. Dual-Porosity Hollow Nanoparticles for the Immunoprotection and Delivery of Nonhuman Enzymes. *Nano Lett.* **2014**, *14 (6)*, 3023–3032.

(18) Ha, W.; Meng, X.-W.; Li, Q.; Fan, M.-M.; Peng, S.-L.; Ding, L.-S.; Tian, X.; Zhang, S.; Li, B.-J. Self-Assembly Hollow Nanosphere for Enzyme Encapsulation. *Soft Matter* **2010**, *6 (7)*, 1405–1408.

(19) Baran, E. T.; Özer, N.; Hasirci, V. *In Vivo* Half Life of Nanoencapsulated L-Asparaginase. *J. Mater. Sci. Mater. Med.* **2002**, *13 (12)*, 1113–1121.

(20) Gaspar, M. M.; Perez-Soler, R.; Cruz, M. E. M. Biological Characterization of L -Asparaginase Liposomal Formulations. *Cancer Chemother. Pharmacol.* **1996**, *38 (4)*, 373–377.

(21) Wan, S.; He, D.; Yuan, Y.; Yan, Z.; Zhang, X.; Zhang, J. Chitosan-Modified Lipid Nanovesicles for Efficient Systemic Delivery of l -Asparaginase. *Colloids Surfaces B Biointerfaces* **2016**, *143*, 278–284.

(22) De, A.; Venkatesh, N. Design and Evaluation of Liposomal Delivery System for L-Asparaginase. *J. Appl. Pharm. Sci.* **2012**, *2 (8)*, 112–117.

(23) Do, T. T.; Do, T. P.; Nguyen, T. N.; Nguyen, T. C.; Vu, T. T. P.; Nguyen, T. G. A. Nanoliposomal L-Asparaginase and Its Antitumor Activities in Lewis Lung Carcinoma Tumor-Induced BALB/c Mice. *Adv. Mater. Sci. Eng.* **2019**, *2019*, 1–8.

(24) Apolinário, A.; Magoń, M.; Pessoa Jr., A.; Rangel-Yagui, C. Challenges for the Self-Assembly of Poly(Ethylene Glycol)–Poly(Lactic Acid) (PEG-PLA) into Polymersomes: Beyond the Theoretical Paradigms. *Nanomaterials* **2018**, *8 (6)*, 373.

(25) Blackman, L. D.; Varlas, S.; Arno, M. C.; Houston, Z. H.; Fletcher, N. L.; Thurecht, K. J.; Hasan, M.; Gibson, M. I.; O'Reilly, R. K. Confinement of Therapeutic Enzymes in Selectively Permeable Polymer Vesicles by Polymerization-Induced Self-Assembly (PISA) Reduces Antibody Binding and Proteolytic Susceptibility. *ACS Cent. Sci.* **2018**, *4 (6)*, 718–723.

(26) Joseph, A.; Contini, C.; Cecchin, D.; Nyberg, S.; Ruiz-Perez, L.; Gaitzsch, J.; Fullstone, G.; Tian, X.; Azizi, J.; Preston, J.; Volpe, G.; Battaglia, G. Chemotactic Synthetic Vesicles: Design and Applications in Blood-Brain Barrier Crossing. *Sci. Adv.* **2017**, *3 (8)*, e1700362.

(27) Simon-Gracia, L.; Hunt, H.; Scodeller, P. D.; Gaitzsch, J.; Braun, G. B.; Willmore, A.-M. A.; Ruoslahti, E.; Battaglia, G.; Teesalu, T. Paclitaxel-Loaded Polymersomes for Enhanced Intraperitoneal Chemotherapy. *Mol. Cancer Ther.* **2016**, *15 (4)*, 670–679.

(28) Pelaz, B.; del Pino, P.; Maffre, P.; Hartmann, R.; Gallego, M.; Rivera-Fernández, S.; de la Fuente, J. M.; Nienhaus, G. U.; Parak, W. J. Surface Functionalization of Nanoparticles with Polyethylene Glycol: Effects on Protein Adsorption and Cellular Uptake. *ACS Nano* **2015**, *9 (7)*, 6996–7008.

(29) LoPresti, C.; Massignani, M.; Fernyhough, C.; Blanazs, A.; Ryan, A. J.; Madsen, J.; Warren, N. J.; Armes, S. P.; Lewis, A. L.; Chirasatitsin, S.; Engler, A. J.; Battaglia, G. Controlling Polymersome Surface Topology at the Nanoscale by Membrane Confined Polymer/Polymer Phase Separation. *ACS Nano* **2011**, *5 (3)*, 1775–1784.

(30) Robertson, J. D.; Rizzello, L.; Avila-Olias, M.; Gaitzsch, J.; Contini, C.; Magoń, M. S.; Renshaw, S. A.; Battaglia, G. Purification of Nanoparticles by Size and Shape. *Sci. Rep.* **2016**, *6 (1)*, 27494.

(31) de Kruijff, R. M.; Raavé, R.; Kip, A.; Molkenboer-Kuenen, J.; Roobol, S. J.; Essers, J.; Heskamp, S.; Denkova, A. G. Elucidating the Influence of Tumor Presence on the Polymersome Circulation Time in Mice. *Pharmaceutics* **2019**, *11 (5)*, 241.

(32) Brinkhuis, R. P.; Stojanov, K.; Laverman, P.; Eilander, J.; Zuhorn, I. S.; Rutjes, F. P. J. T.; van Hest, J. C. M. Size Dependent Biodistribution and SPECT Imaging of 111 In-Labeled Polymersomes. *Bioconjug. Chem.* **2012**, *23 (5)*, 958–965.

(33) Danaei, M.; Dehghankhold, M.; Ataei, S.; Hasanzadeh Davarani, F.; Javanmard, R.; Dokhani, A.; Khorasani, S.; Mozafari, M. Impact of Particle Size and Polydispersity Index on the Clinical Applications of Lipidic Nanocarrier Systems. *Pharmaceutics* **2018**, *10 (2)*, 57.

(34) Wang, L.; Chierico, L.; Little, D.; Patikarnmonthon, N.; Yang, Z.; Azzouz, M.; Madsen, J.; Armes, S. P.; Battaglia, G. Encapsulation of Biomacromolecules within Polymersomes by Electroporation. *Angew. Chemie Int. Ed.* **2012**, *51 (44)*, 11122–11125.

(35) Yealland, G.; Battaglia, G.; Bandmann, O.; Mortiboys, H.

Rescue of Mitochondrial Function in Parkin-Mutant Fibroblasts Using Drug Loaded PMPC-PDPA Polymersomes and Tubular Polymersomes. *Neurosci. Lett.* **2016**, *630*, 23–29.

(36) Aranda-Espinoza, H.; Bermudez, H.; Bates, F. S.; Discher, D. E. Electromechanical Limits of Polymersomes. *Phys. Rev. Lett.* **2001**, *87 (20)*, 208301.

(37) Sueyoshi, D.; Anraku, Y.; Komatsu, T.; Urano, Y.; Kataoka, K. Enzyme-Loaded Polyion Complex Vesicles as *in Vivo* Nanoreactors Working Sustainably under the Blood Circulation: Characterization and Functional Evaluation. *Biomacromolecules* **2017**, *18 (4)*, 1189–1196.

(38) Smith, P. K.; Krohn, R. I.; Hermanson, G. T.; Mallia, A. K.; Gartner, F. H.; Provenzano, M. D.; Fujimoto, E. K.; Goeke, N. M.; Olson, B. J.; Klenk, D. C. Measurement of Protein Using Bicinchoninic Acid. *Anal. Biochem.* **1985**, *150 (1)*, 76–85.

(39) Imada, A.; Igarasi, S.; Nakahama, K.; Isono, M. Asparaginase and Glutaminase Activities of Micro-Organisms. *J. Gen. Microbiol.* **1973**, *76 (1)*, 85–99.

Table of Contents